Short-term automatic forecast algorithm of severe convective cloud identification using FY-2 IR images

LIU Yan'an[1], WEI Ming[2], GAO Wei[1,3], LI Nan[4]

1. *Key Laboratory of Geographic Information Science of Ministry of Education*, *East China Normal University*, *Shanghai* 200062, *China*;
2. *Key Laboratory of Meteorological Disaster of Ministry of Education*, *Nanjing University of Information Science & Technology*, *Nanjing* 210044, *China*;
3. *Natural Resource Ecology Laboratory*, *Colorado State Universtiy*, *Fort Collins CO* 80523, *USA*;
4. *School of Atmospheric Physics*, *Nanjing University of Information Science & Technology*, *Nanjing* 210044, *China*

Abstract: The movement of clouds is qualitative analyzed by forecasters with satellite images currently, which is, however, lack of objectivity and quantitativity. In this paper, based on the stationary satellite infrared (IR) channel (10.3—11.3 μm) images of FY-2C and FY-2D with the time resolution of 15 minutes, brightness temperature (BT) and area threshold are selected to identify the severe convective cloud (SCC). We then use the SCC matching algorithm of maximum correlation to track the short-time automatic prediction of SCC systematically. The experiment results show that the tracking method proposed in this work has higher matching accuracy and efficiency compared with the traditional cross-correlation approach. The cloud center of gravity (CG) extrapolation is markedly superior to the minimum temperature, and the mean temperature, area and roundness all have better indications to the cloud split and merge. Tested by contingency table, the automatic identification and tracking technology has high prediction accuracy and timeliness. In addition, the research of this paper provides a scientific basis for the objective and quantitative application of satellite images to SCC short-time prediction in operation.

Key words: FY-2C and FY-2D, severe convective clouds, cloud threshold identification, maximum correlation tracking algorithm, short-time automatic forecast technology

CLC number: P457.9 **Document code:** A

Citation format: Liu Y A, Wei M, Gao W and Li N. 2012. Short-term automatic forecast algorithm of severe convective cloud identification using FY-2 IR images. Journal of Remote Sensing, 16(1): 79–92

1 INTRODUCTION

Satellite images have become the critical information resources in the weather forecast, which plays an important role in real-time objective analysis and monitoring identification. The characteristics of the meso-scale severe weather (e.g., storms and typhoons) are of rapid occurrence and development, fast movement, and great destructiveness, which show a huge demand for the weather monitoring and forecasting. Doppler radar could monitor the strong convective activity effectively in real-time, but it is expensive, difficult in selecting position, and limited in the monitoring range. While geostationary meteorological satellite can provide all-weather and all day satellite images in large scare, based on satellite images, it is possible to track and warn of the severe convective cloud (SCC) by monitoring the variation and movement of the clouds.

Nowadays, it has been achieved from manual to automatic tracking when using satellite data to identify the clouds. With the area overlapped comparison method, we can realize the automatic tracking for the low cloud top (CT) temperature of infrared (IR) image (Arnaud, et al., 1992). The method of automatically tracking and identifying the meso-scale convective system is achieved based on the maximum spatial correlation tracking technique (Carvalho & Jones, 2001). NCAR has built the Auto-Nowcast system (Mueller, et al., 2003). Bai, et al. (1997) put forward a segment smoothing filter algorithm and threshold algorithm to filter SCC in the infrared image preprocessing, then uses pattern recognition and pattern match technique to trace the SCC. Li (1998) and Liu, et al. (2006) achieved good results in short-term forecast of cloud motion with slowly change using cross-correlation method. Two defects exist in the cross-correlation method: first is that the SCC is always divided into several cells during model calculating, which affects the completeness of the SCC and reduces the matching accuracy

Received: 2011-02-15; **Accepted:** 2011-05-09

Foundation: National Basic Research Program of China (No.2010CB951603); Shanghai Science and Technology Support Program-Special for EXPO (No.10DZ0581600); College Graduate Student Research and Innovation Program of Jiangsu province (No.CX09B_227Z); ECNU Fostering Project (No. PY2011010)

First author biography: LIU Yan'an (1984—), male, graduate student at East China Normal University, his research interests are satellite meteorology and disastrous weather forecast. E-mail: lya163@126.com

Corresponding author biography: WEI Ming (1957—), female, professor, her research interests are atmospheric remote sensing and disastrous weather forecast. E-mail:njueducn@126.com

of the clouds; secondly, this model calculates the whole study area no matter whether the clouds exists or not, which leads to high computing capacity and low efficiency. In this paper, using high temporal resolution satellite images of FY-2C and FY-2D, we put forward an improved maximum correlation method based on the cross-correlation method to realize the matching and tracking of the SCC, and then predict the position, intensity, and location of the SCC in the encounter time.

2 AUTOMATIC IDENTIFICATION, TRACKING AND PREDICTION TECHNOLOGY

2.1 Identification approach

Besides SCC, there are usually other types of cloud clusters or cloud systems mixed at the FY-2 IR images, which can cause uncertainties for the identification and tracking of SCC. This paper adopts the threshold of both BT and area to extract SCC from satellite cloud pictures.

The determination of threshold will affect statistic parameters, such as the life period, beginning position (Vila, et al., 2008). Combined with former research and the characteristics of SCC in the midlatitude region in our country, this paper selects the BT of 235 K as one threshold of SCC (you need to give reference here to support you selection). At the same time, according to the time interval of consecutive satellite images and the average movement speed of cloud clusters, the pixel numbers of SCC at least reached 100 can be identified, namely 2500 km^2 with a spatial resolution of 5 km×5 km.

Parameters of cloud cluster mainly include space, radiation and shape, which can describe the position, intensity and range of SCC. With the evolution of weather, the position, intensity, shape, size and texture feature of SCC change constantly. Through measuring quantitatively the parameters above, the life period of SCC can be determined, ensures the forecast the future state of SCC based on these parameters.

2.1.1 Space parameters

(1) The location of SCC's center of gravity (CG) (X_{CG}, Y_{CG}) is defined as T_B-weighed average,

$$X_{CG}=\frac{\sum_{i=1}^{N_p} X_i T_{Bi}}{\sum_{i=1}^{N_p} T_{Bi}} \quad Y_{CG}=\frac{\sum_{i=1}^{N_p} Y_i T_{Bi}}{\sum_{i=1}^{N_p} T_{Bi}} \tag{1}$$

where X_i, and Y_i are the longitude and latitude of SCC pixel, respectively; T_B is the BT of SCC; N_p is the number of all pixels in SCC.

(2) The location of SCC minimum BT (X_{Tmin}, Y_{Tmin}) is defined as T_{min}-weighed average.

$$X_{T_{min}}=\frac{\sum_{i=1}^{M_p} X_i T_{min\,i}}{\sum_{i=1}^{M_p} T_{min\,i}} \quad Y_{T_{min}}=\frac{\sum_{i=1}^{M_p} Y_i T_{min\,i}}{\sum_{i=1}^{M_p} T_{min\,i}} \tag{2}$$

where X_i, and Y_i are the longitude and latitude of SCC pixels, respectively; T_{min} is the minimum BT of pixels in the SCC. M_p is the number of all pixels equaling to T_{min}.

We can identify the SCC location through both SCC CG and minimum BT, and the deviation between them can be used to judge the offset direction of temperature in SCC. For instance, if the position of CG is located on the left of minimum BT, the temperature of SCC at the east is higher than at the west.

2.1.2 Radiation parameters

(1) The mean temperature of SCC ($\overline{T}$) is defined as the T_B average:

$$\overline{T}=\sum_{i=1}^{N_p}\frac{T_{Bi}}{N_p} \tag{3}$$

(2) The minimum temperature of SCC (T_{min}) is defined as the minimum BT of pixels in the SCC:

$$T_{min}=\mathrm{Min}(T_{Bi}) \tag{4}$$

2.1.3 Shape parameters

(1) The area of SCC (S) is defined by

$$S=k^2\cdot N_P \tag{5}$$

where k is the side length of pixel.

(2) The circumference of SCC (L) is defined by

$$L=k\cdot N_L \tag{6}$$

where N_L is the number of boundary pixels of SCC.

(3) The standard deviation of cloud-top BT (σ_T):

$$\sigma_T=\frac{\sqrt{\sum_{i=1}^{N_p}\left(T_{Bi}-\overline{T}\right)^2}}{N_P} \tag{7}$$

(4) The roundness of SCC ($\boldsymbol{e}$) is defined as the ratio of area and circumference:

$$\boldsymbol{e}=4\pi\times\frac{S}{L^2} \tag{8}$$

which reflects the complexity of the cloud shape. If the shape is closer to round, $\boldsymbol{e}$ is closer to 1; the more complex the shape, the smaller the $\boldsymbol{e}$.

As shown in Fig. 1, regions of all SCC are identified in IR images at the time t_1 and t_2 ($t_2=t_1+\Delta t$, Δt means the time interval) according to both the temperature and area threshold, and the number of SCC identified are M and N, respectively. Regions that do not meet the threshold criteria are set to null value.

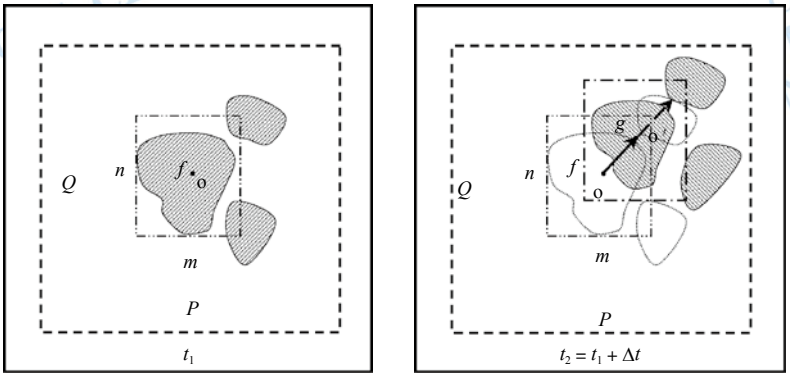

Fig. 1 Schematic diagram of maximum correlation coefficient method

2.2 Tracking algorithm

Based on the maximum correlation between two consecutive IR images, we can judge the location of SCC at the next time. On the basis of cross-correlation coefficient tracking algorithm, maximum correlation coefficient is proposed, and its calculation procedures are shown as below.

Step 1 Region of f^{th} SCC ($1 \leqslant f \leqslant M$) is firstly identified according to the threshold at time t_1, and the CG o represents the center of rectangle covering the SCC, which has a size of $m \times n$, where m and n are the number of pixels in longitude and latitude directions, respectively. Based on the movement speed V of SCC and the time interval Δt of two consecutive IR images, the search range of matching cloud in t_2 IR image is defined as $P \times Q$ ($P \geqslant m$, $Q \geqslant n$),

$$\begin{cases} P = m + 2 \cdot V \cdot \Delta t \\ Q = n + 2 \cdot V \cdot \Delta t \end{cases} \tag{9}$$

which is based on the hypothesis of isotropic movement of all SCC.

Step 2 The search rectangle $m \times n$ traverses N SCC in the regions of P×Q at time t_2 IR image. The correlation coefficient between the f^{th} SCC at time t_1 and the hypothetical matching SCC at time t_2 is given by

$$r = \frac{\sum_{i=1}^{m}\sum_{j=1}^{n}\left(T_f(i,j)-\bar{T}_f\right)\left(T_g(i,j)-\bar{T}_g\right)}{\sqrt{\sum_{i=1}^{m}\sum_{j=1}^{n}\left(T_f(i,j)-\bar{T}_f\right)^2}\sqrt{\sum_{i=1}^{m}\sum_{j=1}^{n}\left(T_g(i,j)-\bar{T}_g\right)^2}} \tag{10}$$

where $\bar{T}_f$, and $\bar{T}_g$ are the mean BT of the f^{th} SCC and hypothetical matching SCC, respectively. Thus, the maximum correlation SCC in search regions is chosen to be the matching SCC of f^{th} SCC.

Step 3 The **Step** 1 and **Step** 2 are repeated until to track all SCC at time t_1.

Compared with cross-correlation method, the maximum correlation algorithm improves both the accuracy and the efficiency of searching matching cloud.

2.3 Forecast method

The time of short-time forecast is defined as 2 hours, and the time interval is 30 min. The forecast indices include location, intensity and range. According to the movement trend of SCC in short-term remaining unchanged in general, the linear least square method is selected to fit a straight line, then forecast the location, intensity and range of SCC in future on the basis of regression equation. There is a reliable forecast result if the SCC has a flat trajectory and keeps the regular movement speed.

3 ALGORITHM TEST

A case of heavy rainfall at the northeast of Hubei province on July 1st, 2008 is chosen. According to the FY-2C images at the time from 16:30 July 1st to 1:30 July 2nd and the FY-2D images from 16:45 July 1st to 1:45 July 2nd, the maximum correlation coefficient method is tested.

The SCC location at the test images must be adjusted before computation due to the spatial matching errors between FY-2C and FY-2D. The displacement deviation of two satellites is computed according to the algorithm proposed by Liu and Wei (2009) to FY-2C, which indicates that about 1—2 pixel errors can be decreased after adjusted along the longitude direction. As shown in Fig. 2, at least 1 pixel relative error can be decreased between FY-2C and FY-2D along the latitude direction.

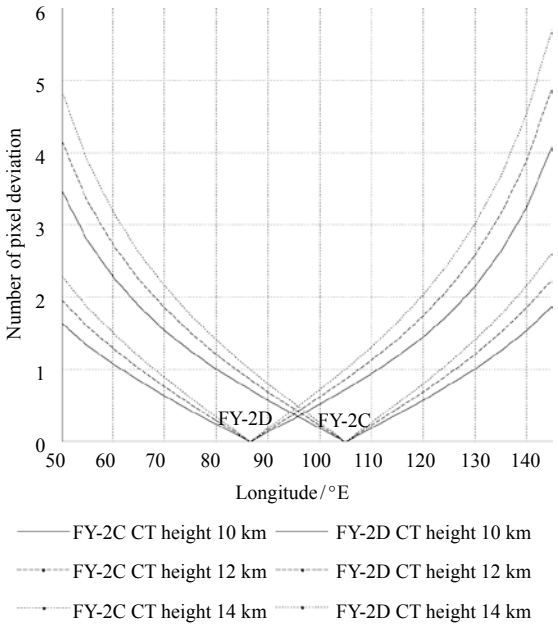

Fig. 2 The displacement deviation curves at the different cloud top (CT) heights along the longitude direction

3.1 Parameters analysis

3.1.1 Space parameters analysis

As shown in Fig. 3 and Fig. 4, the CG of object clouds at FY-2C and FY-2D IR images has a better fitting, and R^2 equal to 0.98 and 0.94, respectively. In contract, the $T_{\min}$ has a poor fitting with R^2 equal of 0.34 and 0.25, respectively. As a result, the CG position of SCC can represent the movement trajectory well, thus the extrapolation using the CG is superior to the $T_{\min}$ when predicting the future position of SCC.

3.1.2 Radiation and shape parameters analysis

According to the splitting and merging process of SCC from 10:00 on July 1st to 01:45 on July 2nd, the evolution of object cloud is divided into four stages, each corresponding to the beginning, development, strengthening and weakening, respectively. As shown in Fig. 5 (a), Fig. 5 (c) and Fig. 5 (d), the mean temperature and area of object cloud are decreased greatly and the roundness increased rapidly from the stage 1 to stage 2, which clearly indicate the splitting process of cloud. The analysis above coincides with the actual situation: the beginning stage the SCC is controlled by two low-temperature centers, then suddenly splits two clouds based on the defined threshold; the lower temperature center cloud is selected to track on the basis of the maximum correlation coefficient, and another cloud is considered as a new cloud which gradually disappears in the follow-up tracking process. At the stage 2, the mean temperature and area of object cloud manifests wide fluctuations, which is consistent with the accumulation of instability energy with the development of cloud. At the stage 3, the mean BT gradually decreases, while at the same time the area increases, which demonstrate the cloud feature of growing luxuriantly. At the stage 4, the object cloud gradually becomes weakened for the raising mean temperature and reducing area. Therefore, in addition to the minimum temperature, the mean temperature, area and round-

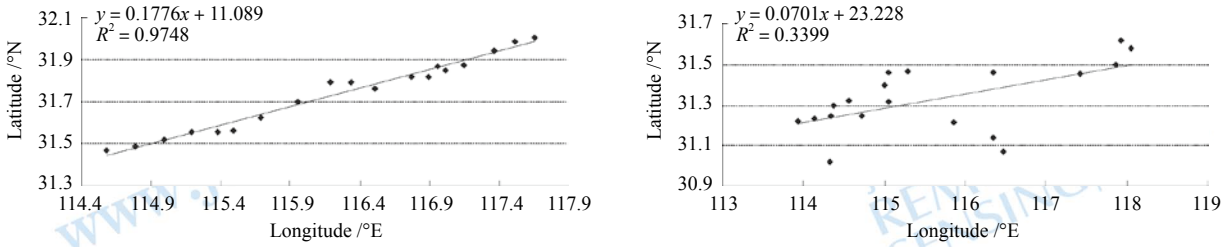

(a) CG scatter diagram of FY-2C (b) Tmin scatter diagram of FY-2C

Fig. 3 Spatial parameters scatter diagram of FY-2C

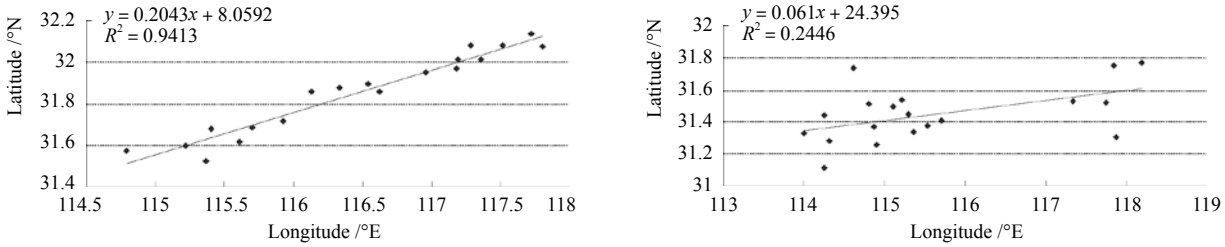

(a) CG scatter diagram of FY-2D (b) Tmin scatter diagram of FY-2D

Fig. 4 Spatial parameters scatter diagram of FY-2D

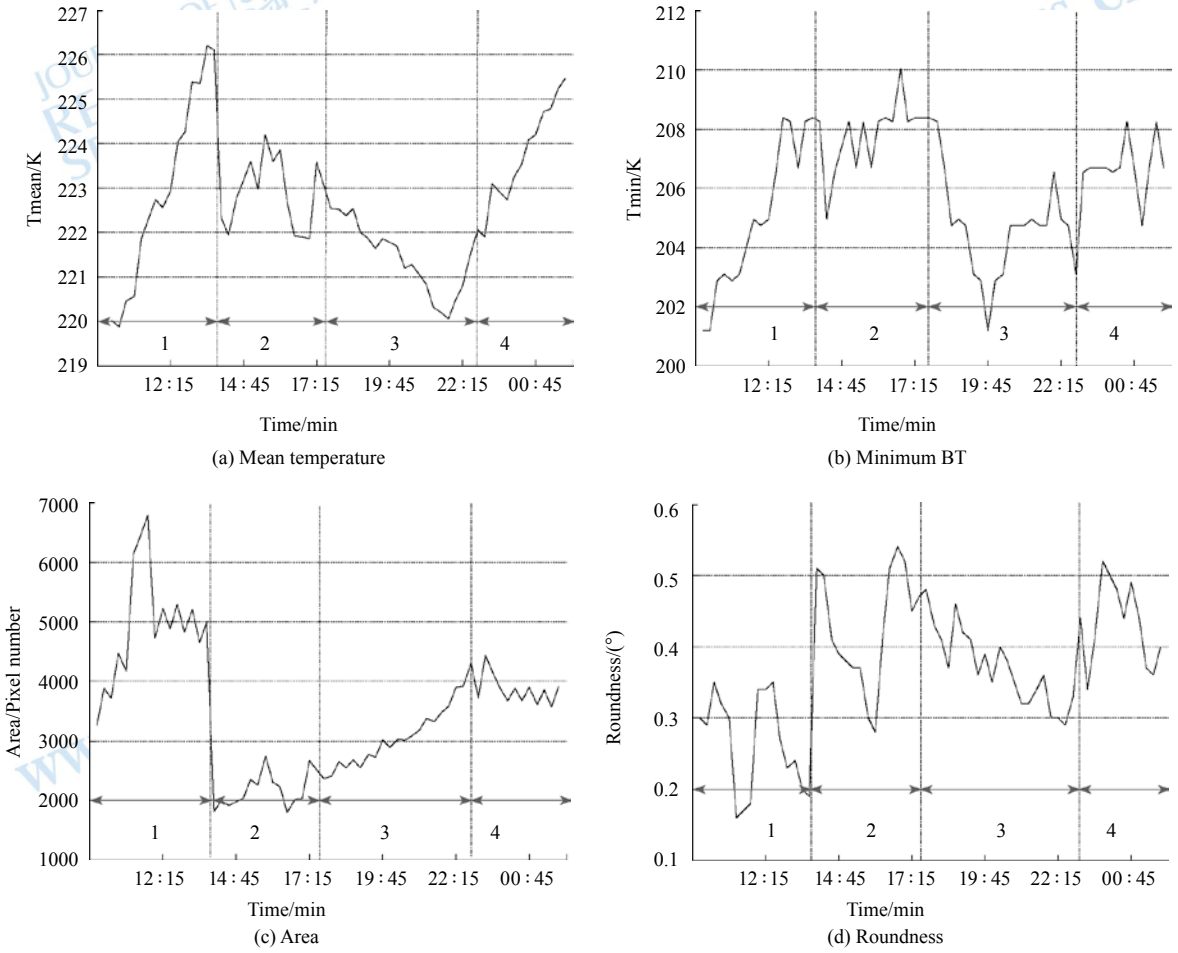

(a) Mean temperature (b) Minimum BT

(c) Area (d) Roundness

Fig. 5 Evolution line of the SCC at the time interval of 15 min

ness can reflect the evolution of cloud, and have an indicative effect to judge the various stage of cloud.

3.2 Verification of tracking

The tracking maps of rainstorm clouds are shown in Fig. 6 from 16:30 to 22:00 on July 1st, 2008. The SCC are identified firstly based on the threshold at the FY-2C IR images. From the tracking maps, we know the CG of SCC (shown as black point) is moving to northeast, and the minimum temperature gradually decreases while the area increases, which demonstrate the clouds are becoming stronger. Accordingly, the identification and tracking method in this paper are convenient and effective.

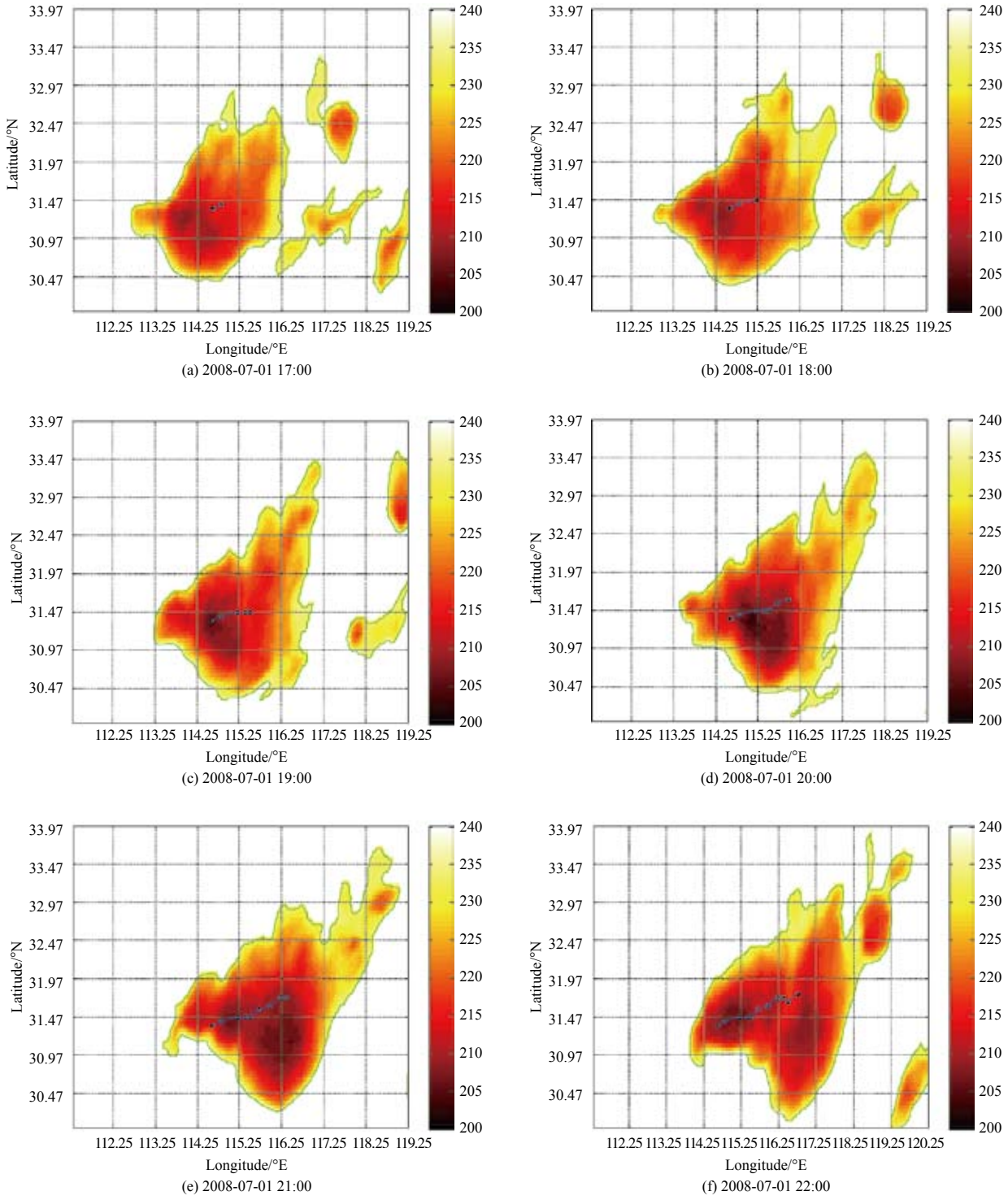

Fig. 6 Tracking maps of rainstorm cloud at the northeast of Hubei province on July 1st, 2008

3.3 Verification of forecast

3.3.1 Testing intensity and range

The evolution of SCC mean temperature from the time of 17:45 to 21:00 is shown in Fig. 7 (a), where the solid line represents the true value. The dotted line indicates the forecast on the basis of least square method using FY-2C and FY-2D data at the interval of 15 min, and the forecast time is 30 min, 60 min, 90 min and 120 min, respectively. At the same time the true area evolution and the forecast of SCC are shown in Fig. 7 (b). Accordingly, the forecast of cloud mean temperature and area are in accordance with the observation of satellite, and the forecast results explain the cloud at the stage of strong development.

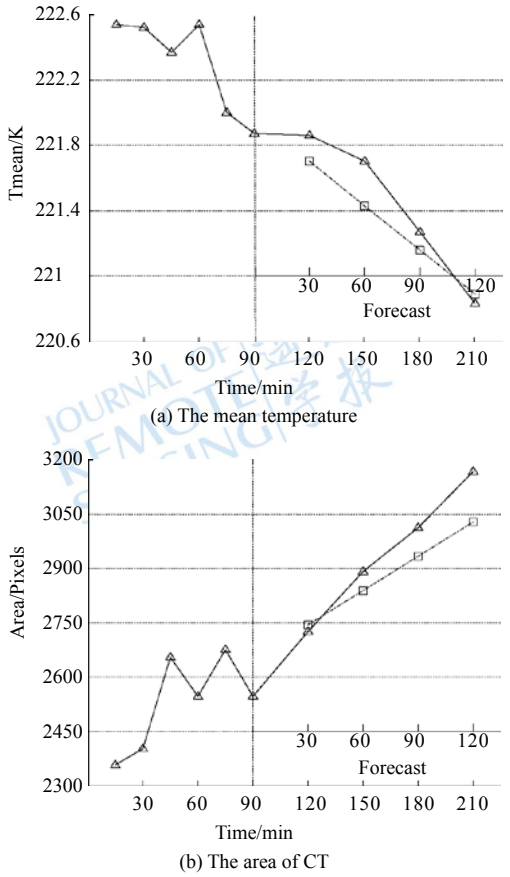

Fig. 7 The forecast of intensity and range of SCC (The solid line means the observation, and the dotted line means the forecast)

3.3.2 Testing location

The contingency table method is used to quantitatively assess the forecast of SCC (Wilks, 1995). We consider the forecast pixel as success if the predicted value and the observed value are both lesser or equal to the threshold ($T_{obs} \leqslant 235$ K, $T_{pre} \leqslant 235$ K); consider as miss if $T_{obs} \leqslant 235$ K and $T_{pre} > 235$ K; consider as fail if $T_{obs} > 235$ K and $T_{pre} \leqslant 235$ K. Thus, the probability of detection (POD), false alarm ratio (FAR) and critical success index (CSI) are defined as:

$$\mathrm{POD} = \frac{n_{\mathrm{sucess}}}{n_{\mathrm{sucess}} + n_{\mathrm{miss}}} \tag{11}$$

$$\mathrm{FAR} = \frac{n_{\mathrm{fail}}}{n_{\mathrm{sucess}} + n_{\mathrm{fail}}} \tag{12}$$

$$\mathrm{CSI} = \frac{n_{\mathrm{success}}}{n_{\mathrm{success}} + n_{\mathrm{miss}} + n_{\mathrm{fail}}} \tag{13}$$

where POD, FAR and CSI are between 0—1. Higher POD and CSI indicate more accurate of the forecast and smaller FAR also stands better forecast.

Table 1 The nowcasting skill of FY-2C

Skill	30 min	60 min	90 min	120 min
POD	0.77	0.65	0.55	0.43
FAR	0.19	0.29	0.37	0.47
CSI	0.65	0.52	0.41	0.31

Table 2 The nowcasting skill of FY-2D

Skill	30 min	60 min	90 min	120 min
POD	0.80	0.67	0.58	0.49
FAR	0.17	0.26	0.33	0.41
CSI	0.69	0.55	0.45	0.37

As shown in Table 1 and Table 2, the forecasting POD of FY-2C and FY-2D after 30 minutes reaches 0.77 and 0.88, respectively, while FAR are only 0.19, 0.17. This indicates 80% pixels are predicted rightly and 17% are incorrectly for FY-2D IR images. Therefore, the nowcasting of SCC essentially achieves the desired effect, but the precision gradually reduces with the growth of time.

3.3.3 Relation between CT BT and precipitation

As shown in Fig. 8, CT BT has a good relationship with the 1 h average precipitation measured by rain gauge, and lower CT BT is corresponded to more precipitation. As a result, once automatic identification, tracking and prediction methods meet the accuracy of operation need, we can predict the basic characteristics of heavy rainfall in future by taking account of the result of SCC forecast.

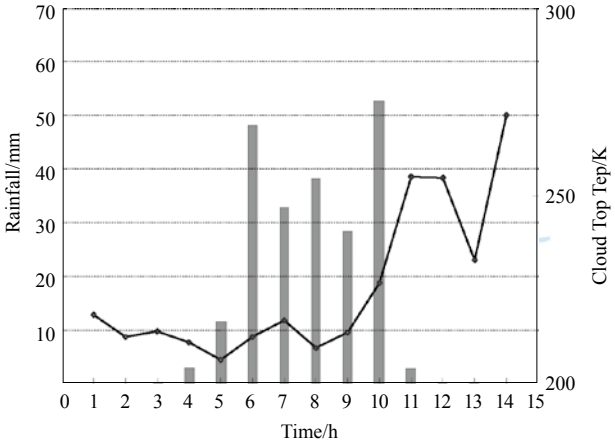

Fig. 8 The relation between the observation of rain gauge and the corresponded BT. (The histogram means the precipitation, and the line means the BT of CT) July 1, 2008 UTC (Stn 57398)

4 CONCLUSIONS

Based on high temporal resolution satellite images provided by FY-2C and FY-2D satellites, maximum correlation coefficient method is proposed to achieve the identification, matching, tracking and prediction of SCC. Tested by the contingency table method, our method shows satisfied forecast results and higher matching accuracy and efficiency than cross correlation coefficient method. Studies have demonstrate that using CG of cloud to predict the location of clouds can be superior to the minimum BT method while combining the average BT, area and circularity can play good instruction in determining the development stage of cloud. This paper provides the basic theory and methods to identifying, tracking, matching and quantitative predicting high intensity cloud by using satellite imageries.

Acknowledgements: Thanks to Hubei Meteorological Bureau offer the precipitation data of rain gauge and National Satellite Meteorological Center offer the FY-2C and FY-2D IR images at the service network of Fengyun satellite remote sensing data.

REFERENCES

Arnaud Y, Desbois M and Maizi J. 1992. Automatic tracking and characterization of African convective systems on Meteosat pictures. Journal of Applied Meteorology, 31(5): 443–453 DOI: 10.1175/1520-0450(1992)031<0443:ATACOA>2.0.CO;2

Bai J, Wang H Q and Tao Z Y. 1997. Recognition and tracing of severe convective cloud from IR Images of GMS. Journal of Tropical Meteorology, 13(2): 158–167

Carvalho L M V and Jones C. 2001. A satellite method to identify structural properties of mesoscale convective systems based on maximum spatial correlation tracking technique (MASCOTTE). Jounal of Applied Meteorology, 40(10): 1683-1701 DOI: 10.1175/1520–0450(2001)040<1683:ASMTIS>2.0.CO;2

Li Z J. 1998. Estimation of cloud motion using cross-correlation. Advance in Atmospheric Sciences, 15(2): 277-282 DOI: 10.1007/s00376–998–0046–0

Liu K F, Zhang R and Sun Z B. 2006. A cloud movement short-time forecast based on cross-correlation. Journal of Image and Graphics, 11(4): 586–591

Liu Y A and Wei M. Application of FY-2C Data in Rainstorm Nowcasting. The First International Conference on Information Science and Engineering. 2009: 4766–4769 DOI: 10.1109/ICISE.2009.329

Mueller C, Saxen T, Roberts R, Wilson J, Betancourt T, Dettling S, Oien N and Yee J. 2003. NCAR Auto-Nowcast System. Weather and Forecasting, 18(4): 545–561 DOI: 10.1016/S0040-4020(97)10144-2

Vila D A, Machado L A T, Laurent H and Velasco I. 2008. Forecast and tracking the evolution of cloud clusters (ForTraCC) using satellite infrared imagery: methodology and validation. Weather and Forecasting, 23(2): 233–245 DOI: 10.1175/2007WAF2006121.1

Wilks D S. 2005. Statistical Methods in the Atmospheric Sciences: An Introduction. 2nd ed. Academic Press: 467

FY-2红外云图中强对流云团的短时自动预报算法

刘延安[1]，魏鸣[2]，高炜[1,3]，李南[4]

1. 华东师范大学 地理信息科学教育部重点实验室，上海 200062；
2. 南京信息工程大学 气象灾害省部共建教育部重点实验室，江苏 南京 210044；
3. 美国科罗拉多州立大学 自然资源生态实验室，美国 柯林斯堡 80523；
4. 南京信息工程大学 大气物理学院，江苏 南京 210044

摘 要：目前气象预报业务中，预报员主要借助卫星云图，定性判断云团的移动趋势，缺乏形式化的定量评判方法。本文基于FY-2C与FY-2D的高时间分辨率的近红外影像(10.3—11.3 μm)，采用亮温和面积阈值方法进行云团识别，然后根据最大相关系数云团匹配技术进行追踪，系统地实现强对流云团的自动临近预测。实验结果表明，本文提出的最大相关系数追踪比传统的交叉相关系数法具有更高的匹配精度和运行效率,而且研究发现云团质心外推明显优于最低亮温外推，平均亮温、面积、圆形度对云团的分裂合并有较好的指示作用，经列联表法检验，本文提出的自动识别追踪技术具有较高预测精度和预测时效，并且为卫星云图业务化应用提供了定量科学依据。

关键词：FY-2C和FY-2D，强对流云团，云团阈值识别，最大相关系数追踪算法，自动临近预测技术

中图分类号：P457.9 **文献标志码**：A

引用格式：刘延安，魏鸣，高炜，李南. 2012. FY–2红外云图中强对流云团的短时自动预报算法. 遥感学报，16(1): 79–92
Liu Y A, Wei M, Gao W and Li N. 2012. Short-term automatic forecast algorithm of severe convective cloud identification using FY-2 IR images. Journal of Remote Sensing, 16(1): 79–92

1 引 言

在气象预报业务中，卫星云图已成为关键的信息资源，在实时客观分析和监测识别等领域，卫星云图发挥了重要作用。暴雨和台风等中小尺度灾害性天气具有发生发展快、移动迅速、破坏性强等特点，对此类灾害性天气的监测预报十分重要。多普勒雷达能够实时、有效地监测强对流活动，但成本昂贵，布点困难，监测范围有限。静止气象卫星能够提供大范围、全天候卫星云图信息，基于此类云图可以把握云团变化和移动趋势，实现对强对流云团的实时追踪和预警。

目前，利用卫星资料实现对云团的识别追踪研究，已实现了从人工追踪向自动追踪的转变。例如：利用红外卫星云图，采用面积重叠比较法，实现了低温云顶云团的自动追踪(Arnaud 等，1992)；利用最大空间相关追踪技术，实现了对中尺度对流系统的自动识别与追踪(Carvalho和Jones，2001)；NCAR建立的自动临近预报系统(Mueller 等，2003)；利用区域平滑滤波和阈值剔除相结合的强对流云团过滤算法，过滤出强对流云团，应用模式识别和模式匹配技术追踪强对流云团(白洁 等，1997)；利用交叉相关法，实现对平稳云团的短时外推预测(Li，1998；刘科峰 等，2006)。交叉相关系数法存在两个缺陷：一是模型计算时，经常将一个强对流云团划分成几个小区，破坏了强对流云团的整体性，降低了云团匹配精度；二是不论研究区内是否存在云团，该模型都面向整个研究区展开计算，计算量大，效率较低。本文利用FY-2C和FY-2D监测的高时间分辨率卫星云图资料，基于交叉相关系数法，提出了改进的最大相关系数法，实现了强对流云团的匹配追踪，预报了强对流云团未来时刻的位置、强度和分布范围。

收稿日期：2011-02-15；**修订日期**：2011-05-09

基金项目：国家重点基础研究发展计划(编号: 2010CB951603)；上海市科委世博科技专项(编号: 10DZ0581600)；江苏省普通高校研究生科研创新计划(编号: CX09B_227Z)；华东师大优博培育行动计划(编号: PY2011010)

第一作者简介：刘延安(1984—)，男，博士研究生，从事卫星气象学和灾害性天气预报研究。E-mail: lya163@126.com。

通信作者简介：魏鸣(1957—)，女，教授，博士生导师，主要从事大气遥感与灾害性天气预测研究。E-mail: njueducn@126.com。

2 自动识别、追踪和预测技术

2.1 强对流云团的识别算法

在FY-2红外云图上，除了强对流云团外，常常还混有其他类型云团或云系。这些云团或云系给强对流云团的识别和追踪带来了困难。本文采用亮温阈值和面积阈值，将强对流云团从卫星云图中剥离出来。

选取的阈值将影响强对流云团的生命期、起始位置等统计参数(Vila 等，2008)，结合以往研究和中国中纬度地区强对流特征，文中将强对流云团的云顶亮温阈值选定为235 K；根据云图时间间隔和云团移动速度，将强对流云团的最小面积阈值选定为100个像元(分辨率为5 km × 5 km)，即2500 km^2。

云团参数通常包括空间、辐射和形状等参数，可以描述云团的位置、强度和范围。随着天气过程的发展，红外云图中的强对流云团位置、强度、形状、大小和纹理等特征参数均会不断变化。通过定量测算上述参数，可以确定云团所处生命期状态。

2.1.1 空间参数

(1)云团质心位置(X_{CG}, Y_{CG})：

$$X_{CG}=\frac{\sum_{i=1}^{N_P}X_iT_{Bi}}{\sum_{i=1}^{N_P}T_{Bi}} \qquad Y_{CG}=\frac{\sum_{i=1}^{N_P}Y_iT_{Bi}}{\sum_{i=1}^{N_P}T_{Bi}} \tag{1}$$

式中，X_i，Y_i分别为像元的经度和纬度；T_B为像元亮温值；N_P为云团内所有像元的个数。

(2)最低亮温位置($X_{T_{min}}$，$Y_{T_{min}}$)：

$$X_{T_{min}}=\frac{\sum_{i=1}^{M_P}X_iT_{\min i}}{\sum_{i=1}^{M_P}T_{\min i}} \qquad Y_{T_{min}}=\frac{\sum_{i=1}^{M_P}Y_iT_{\min i}}{\sum_{i=1}^{M_P}T_{\min i}} \tag{2}$$

式中，X_i，Y_i分别为像元的经度和纬度；T_{min}为云团内像元最低亮温值；M_P为亮温值等于T_{min}的像元个数。

云团质心位置与最低亮温位置都可以标识暴雨云团的位置，两者间偏差可以用来判断暴雨云团温度的偏移方向。例如，质心位于最低亮温中心的右侧，表明暴雨云团的冷区偏向西侧，即云团东侧温度高于西侧。

2.1.2 辐射参数

(1)云顶平均亮温 $\overline{T}$：

$$\overline{T}=\sum_{i=1}^{N_p}\frac{T_{Bi}}{N_p} \tag{3}$$

(2)云顶最低亮温T_{min}：

$$T_{min}=\mathrm{Min}(T_{Bi}) \tag{4}$$

2.1.3 形状参数

(1)云团面积S(单位：km^2)

$$S=k^2\cdot N_P \tag{5}$$

(2)云团周长L(单位：km)

$$L=k\cdot N_L \tag{6}$$

式中，N_L为云团边界像元点个数。

(3)云顶亮温标准差σ_T：反映云团的密集和扩散程度。

$$\sigma_T=\frac{\sqrt{\sum_{i=1}^{N_P}\left(T_{Bi}-\overline{T}\right)^2}}{N_P} \tag{7}$$

(4)云团圆形度$\boldsymbol{e}$：反映云团轮廓的复杂度。

$$\boldsymbol{e}=4\pi\times\frac{S}{L^2} \tag{8}$$

式中，S为面积，L为周长。若云团轮廓越接近圆形，$\boldsymbol{e}$越接近1；轮廓越复杂，$\boldsymbol{e}$越小。

如图1所示，借助亮温阈值和面积阈值，识别出t_1和t_2时刻($t_2=t_1+\Delta t$，Δt代表时间间隔)云图内的所有强对流云团，云团数分别为M和N。除强对流云团外，其他像元均赋为“Nodata”。

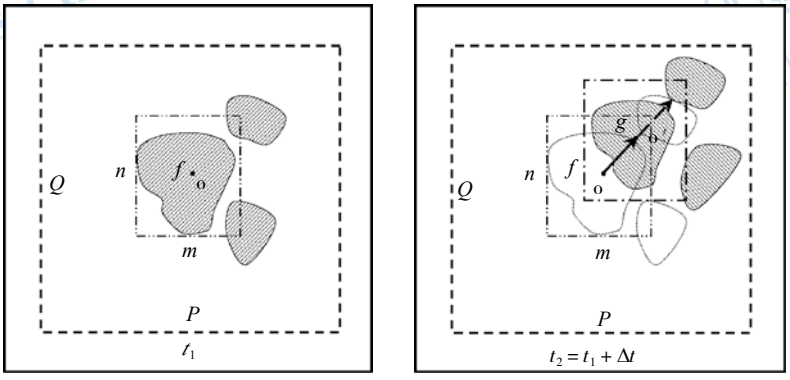

图1 最大相关系数法示意图

2.2 强对流云团的追踪算法

针对两幅连续的卫星云图，通过计算两幅云图中强对流云团相关系数，分析目标云团间的关系密切程度，判断目标云团下一时刻所处位置。文中以交叉相关系数追踪法为基础，提出最大相关系数追踪法，计算步骤如下：

步骤1 在t_1时刻卫星云图上，测算f云团($1\leqslant f\leqslant M$)的范围。如果以f云团质心o为中心，覆盖云团的矩形的经度方向有m个像元数，纬度方向有n个像元数，则f云团的范围可以表示为$m\times n$；根据云团的移动速度V和连续两幅云图的时间间隔Δt，确定在t_2时刻云图上匹配云团的搜索范围为$P\times Q(P\geqslant m,Q\geqslant n)$，$P=m+2\times V\cdot\Delta t$，$Q=n+2\times V\cdot\Delta t$，设置范围时假设云团移动时各向等性。

步骤2 令t_1时刻$m\times n$区域代表f云团，$T_f(i,j)$为f云团的云顶亮温数据集。令t_2时刻的搜索窗口为$m\times n$，窗口需遍历$P\times Q$区域内N个云团，$T_g(i,j)$代表假想匹配云团g的云顶亮温数据集。$1\leqslant i\leqslant m$，$1\leqslant j\leqslant n$，代表云团的行列号，根据下式可以分别计算f云团与假想匹配云团间的相关系数。

$$r=\frac{\sum_{i=1}^{m}\sum_{j=1}^{n}\left(T_f(i,j)-\bar{T}_f\right)\left(T_g(i,j)-\bar{T}_g\right)}{\sqrt{\sum_{i=1}^{m}\sum_{j=1}^{n}\left(T_f(i,j)-\bar{T}_f\right)^2}\sqrt{\sum_{i=1}^{m}\sum_{j=1}^{n}\left(T_g(i,j)-\bar{T}_g\right)^2}} \tag{9}$$

式中，$\bar{T}_f$和$\bar{T}_g$分别为f云团和假想匹配云团g的平均亮温。

将t_2搜索区域中与t_1时刻f云团相关系数最大的假想匹配云团作为t_2时刻与t_1时刻f云团相匹配的g云团。

步骤3 选取t_1时刻云图中下一个目标云团，重复**步骤1**和**步骤2**，找到匹配云团，重复这一过程，直至追踪完所有对流云团。

与交叉相关系数法比较，此法改善了云团匹配准确度，提高了云团匹配搜索效率。

2.3 强对流云团的预测

将临近预报的时效定为2 h，预报时间间隔定为30 min。选取的预报指标包括：位置、强度和范围。根据短时内强对流云团基本趋向于直线的移动特点，采用最小二乘法对上述预报指标分别进行线性拟合，并依据回归方程，预测未来时刻强对流云团的位置、强度和范围。对于具有平直移动轨迹和稳定平移速度的强对流云团，预报结果比较可靠。

3 效果检验

本文结合2008年7月1日湖北鄂东北的一次特大暴雨过程，利用FY-2C 2008年7月1日16:30—7月2日01:30的影像和FY-2D 2008年7月1日16:45—7月2日01:45的影像，对最大相关系数法进行了模拟检验。

由于FY-2C和FY-2D云图空间位置存在匹配误差，计算前必须对试验影像进行几何校正，根据Liu和Wei(2009)对FY-2C云顶像元位移偏差校正处理算法得到两星经度方向上的云顶位移偏差(见图2)。在中纬度地区，校正影像在经线方向可以减少1—2个像元的误差，在纬线方向可降低两星之间1个像元以上的误差。

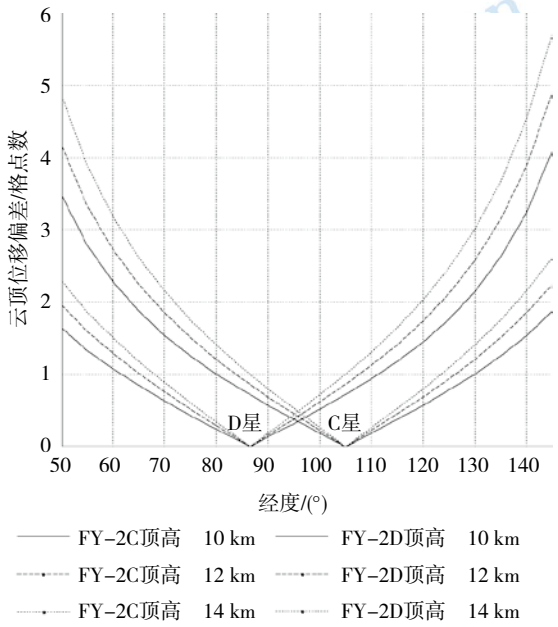

图2 FY-2C、FY-2D卫星经度方向云顶位移偏差

3.1 云团参数分析

3.1.1 空间参数

从图3和图4可以看出，在FY-2C和FY-2D的卫星云图中，目标云团质心位置的经度和纬度之间线性拟合关系非常好，R^2分别为0.98和0.94；目标云团最低亮温位置的经度和纬度之间线性拟合关系不理想，R^2分别仅为0.34和0.25。说明目标云团质心较好地反映了目标云团的移动轨迹，对目标云团进行位置预测时，云团质心位置明显优于云团最低亮温位置。

3.1.2 辐射参数和形状参数

根据2008年7月1日10:00—7月2日01:45暴雨过程中云团的分裂合并情况，将目标云团的演化过程分为4个阶段，分别对应目标云团的起始、发展、旺盛和减弱4个过程。从图5(a)(c)(d)中可以看出，从阶段1转化为阶段2的过程中，目标云团的平均亮温和面积急剧降低，而圆形度急剧增加，很好地表示出目标云团的分裂过程，起始阶段云团一直由双低温中心控制，

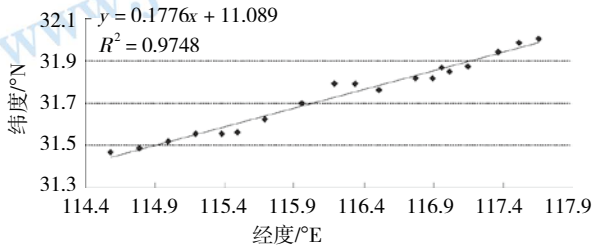

(a) FY-2C质心位置散点图

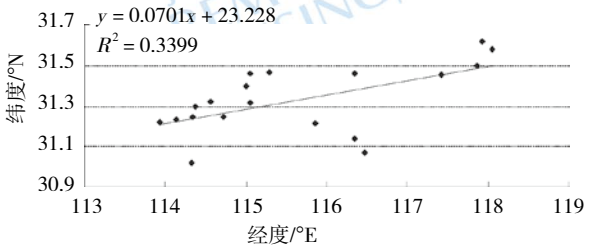

(b) FY-2C最低亮温位置散点图

图3 FY-2C云团空间参数散点拟合图

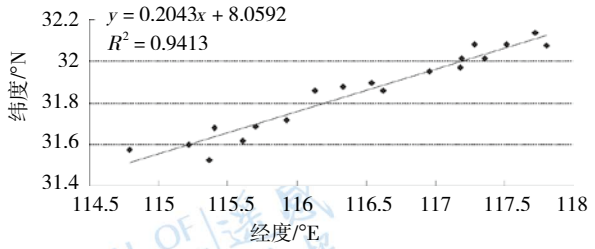

(a) FY-2D质心位置散点图

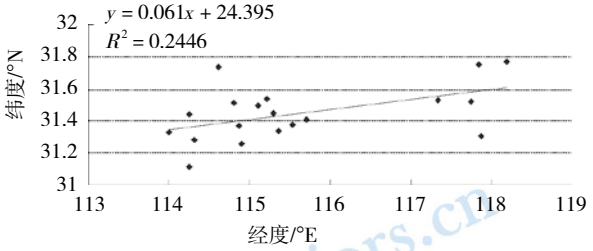

(b) FY-2D最低亮温位置散点图

图4 FY-2D云团空间参数散点拟合图

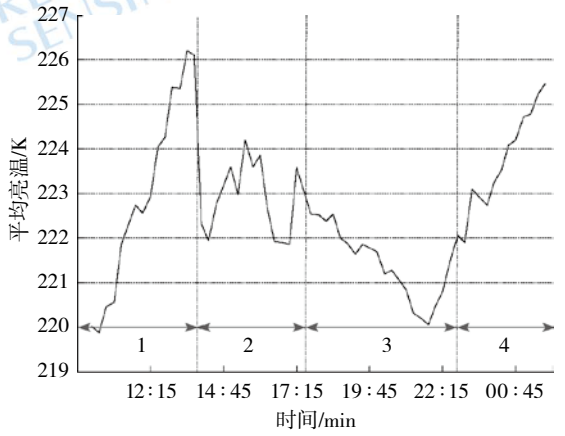

(a) 平均亮温

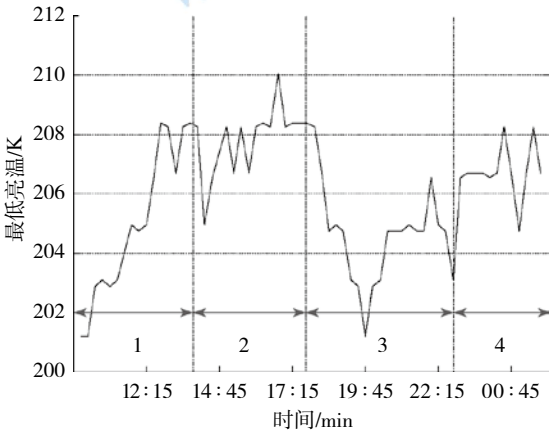

(b) 最低亮温

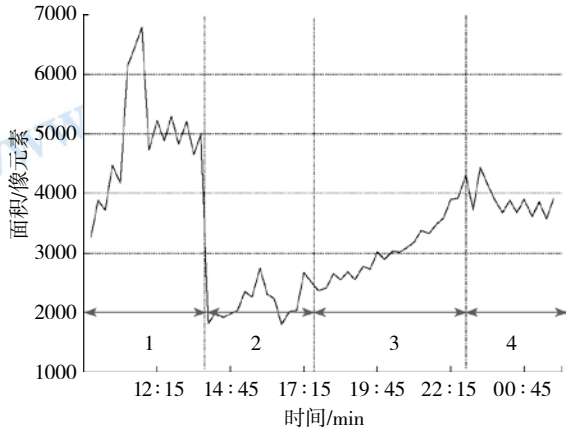

(c) 面积

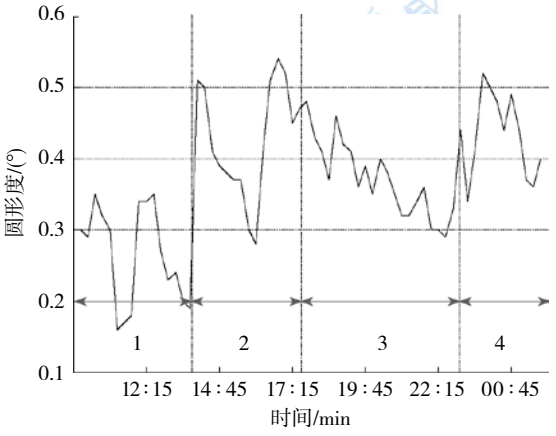

(d) 圆形度

图5 暴雨云团15 min间隔的演化折线图

该阶段突变正好为两中心分裂，根据最大相关系数追踪较强低温中心云团，而另一较弱低温中心作为新生云团，后续追踪过程中逐渐消失；在阶段2，目标云团的平均亮温、面积有较大波动，这与云团发展过程中不稳定能量聚集过程一致；在阶段3，云团平均亮温逐渐变低，面积逐渐增大，很好地反映了目标云团发展旺盛特征；在阶段4，云团平均亮温变高，面积逐渐变小，表现出目标云团有强转弱的特征。事实说明，除最低亮温外，云团平均温度、面积和圆形度能较好反映云团发展演化过程，对判断云团发展阶段具有指示作用。

3.2 追踪效果检验

图6是FY-2C云图2008-07-01 16:30—22:00的6次

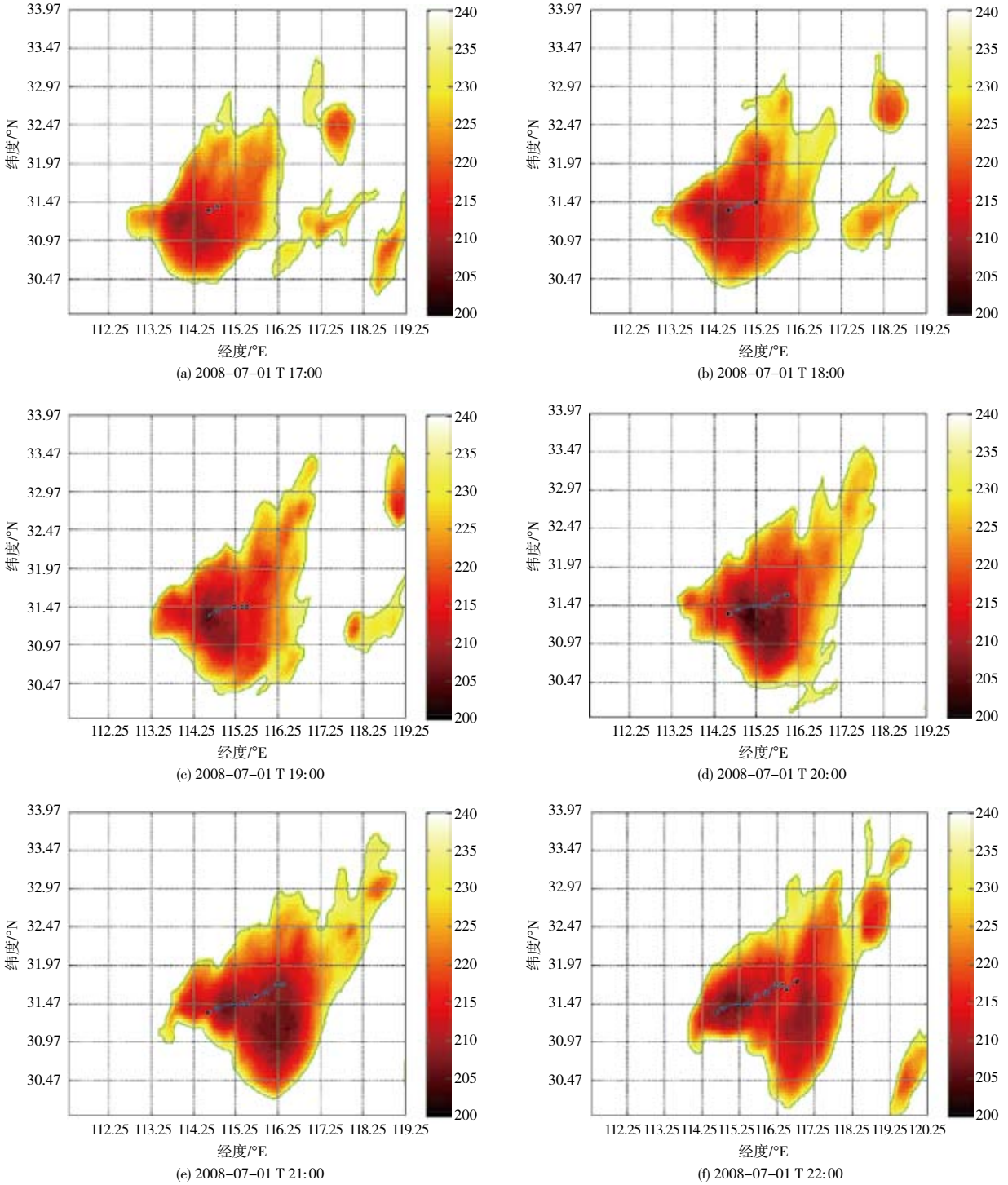

(a) 2008–07–01 T 17:00
(b) 2008–07–01 T 18:00
(c) 2008–07–01 T 19:00
(d) 2008–07–01 T 20:00
(e) 2008–07–01 T 21:00
(f) 2008–07–01 T 22:00

图6 2008-07-01 湖北鄂东北暴雨云团的追踪

整点时刻最强暴雨云团的追踪路径图。根据T-R阈值对研究范围内云团进行识别，团中黑点分别为各个时刻的云团质心，可以看出云团质心向东北方向发展，云团的最低亮温逐渐变低，面积逐渐增大，说明云团正发展增强。从追踪的效果看，云团识别和追踪方法便捷有效。

3.3 预报效果检验

3.3.1 对流云团强度和范围

图7(a)显示了2008-07-01鄂东北强对流云团平均亮温在17:45—21:00的演化过程，其中，实线为实际过程折线，虚线为FY-2C和FY-2D两星15 min间隔数据的

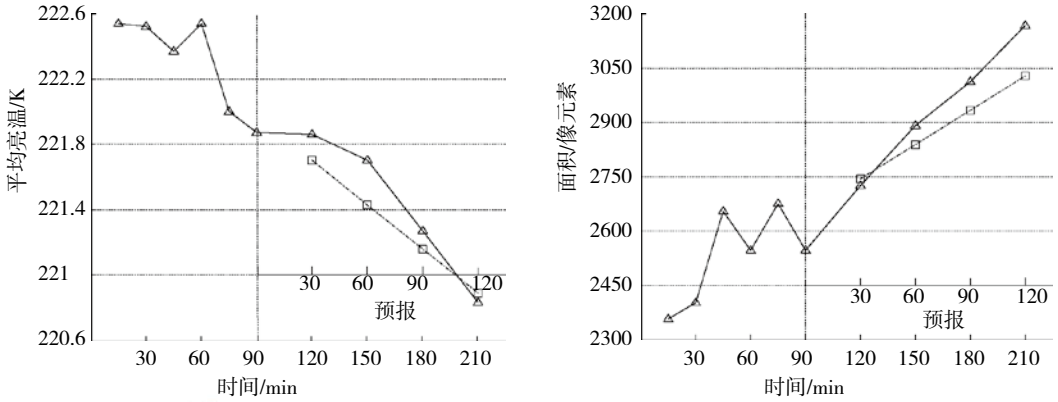

(a) 云顶平均亮温　　(b) 云顶面积

图7 暴雨云团强度和范围预测(实线为实测值，虚线为预测值)

最小二乘线法预测过程折线。预报时点为30 min，60 min，90 min和120 min。图7(b)为同时段的目标云团的面积变化过程和预测曲线。可以看出，平均亮温和面积预测基本与实测值相符，预测结果说明云团正处于发展旺盛阶段。

3.3.2 对流云团位置

采用列联表法对位置预报结果进行定量评价(Wilks，1995)。将预报的像元值和实际观测的像元值进行对比，如果实测像元值和预报像元值均小于等于阈值($T_{实际}$≤235 K，$T_{预报}$≤235 K)，则认为该像元预报成功；如果实测像元值小于等于阈值，而预报像元值大于阈值($T_{实际}$≤235 K，$T_{预报}$>235 K)，则该像元是漏报；如果实测像元值大于阈值，而预报像元值小于等于阈值($T_{实际}$>235 K，$T_{预报}$≤235 K)，则该像元是虚报。分别计算探测比(POD)、虚报比(FAR)和临界成功指数(CSI)。

$$\mathrm{POD}=\frac{n_{成功}}{n_{成功}+n_{漏报}} \tag{10}$$

$$\mathrm{FAR}=\frac{n_{虚报}}{n_{成功}+n_{虚报}} \tag{11}$$

$$\mathrm{CSI}=\frac{n_{成功}}{n_{成功}+n_{漏报}+n_{虚报}} \tag{12}$$

式中，POD、FAR和CSI的数值都介于0—1之间，如果POD和CSI越大，则预报越准确；如果FAR越小，则预报越准确。

表1 FY-2C云图预报评价结果

评价指标	30 min	60 min	90 min	120 min
POD	0.77	0.65	0.55	0.43
FAR	0.19	0.29	0.37	0.47
CSI	0.65	0.52	0.41	0.31

表2 FY-2D云图预报评价结果

评价指标	30 min	60 min	90 min	120 min
POD	0.80	0.67	0.58	0.49
FAR	0.17	0.26	0.33	0.41
CSI	0.69	0.55	0.45	0.37

从表1和表2可以看出，FY-2C和FY-2D的30 min预报的POD分别达到0.77、0.80，而FAR分别在0.19、0.17左右。就FY-2D云图而言，80%像素被准确预测，17%的预测结果为虚报，说明对目标云团的短时位置预报基本能达到了预期效果。如果时间增长，预测精度将逐渐下降。

3.3.3 云顶平均亮温与降水

雨量站实测的1 h降水量与云顶平均亮温存在很好的对应关系(见图8)，云顶亮温越低，降水越多。说明自动识别、追踪和预测技术一旦满足业务精度需

求，则利用强对流云团的预测结果，能够掌握未来时刻强降水的基本特征。

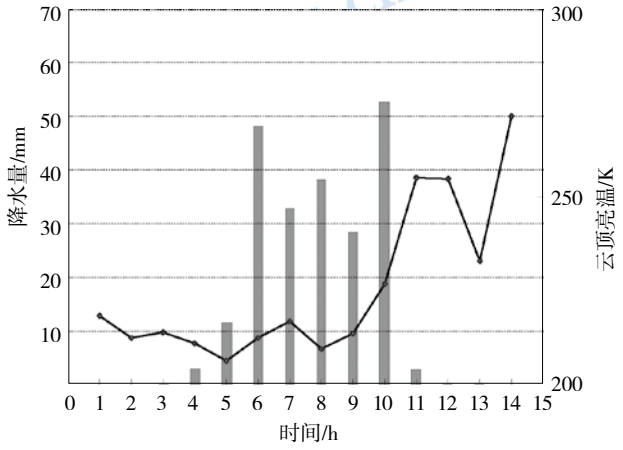

图8 雨量站点1 h降水量与对应云图TBB的关系
(世界标准时间2008–07–01，测试站点的编号为57398，柱状图表示降水量，折线图表示云顶亮温)

4 结 论

本文基于中国的FY-2C和FY-2D两颗卫星提供的高时间分辨率卫星云图，针对强对流云团的检测预报，提出了最大相关系数法，实现了强对流云团的识别、匹配、跟踪和预报，经列联表法检验，证明该方法能够获得较为满意的预报效果。最大相关系数比交叉相关系数法具有更高的匹配精度和运行效率。研究表明，对云团位置进行预报时，采用云团质心较最低亮温更为优越，平均亮温、面积和圆形度组合使用时，对判断云团的发育阶段有较好指示作用。此项研究为基于气象卫星云图开展高强度云团识别、跟踪、匹配、预报的定量业务工作，提供了应用基础理论和方法。

志 谢 感谢湖北省气象局提供实测降水资料和中国气象局国家气象卫星中心风云卫星遥感数据服务网提供的FY−2C和FY−2D卫星数据。

参考文献(References)

Arnaud Y, Desbois M and Maizi J. 1992. Automatic tracking and characterization of African convective systems on Meteosat pictures. Journal of Applied Meteorology, 31(5): 443–453 DOI: 10.1175/1520–0450(1992)031<0443:ATACOA>2.0.CO;2

白洁, 王洪庆, 陶祖钰. 1997. GMS卫星红外云图强对流云团的识别与追踪. 热带气象学报, 13(2): 158–167

Carvalho L M V and Jones C. 2001. A satellite method to identify structural properties of mesoscale convective systems based on maximum spatial correlation tracking technique (MASCOTTE). Jounal of Applied Meteorology, 40(10): 1683–1701 DOI: 10.1175/1520–0450(2001)040<1683:ASMTIS>2.0.CO;2

Li Z J. 1998. Estimation of cloud motion using cross-correlation. Advance in Atmospheric Sciences, 15(2): 277–282 DOI: 10.1007/s00376–998–0046–0

刘科峰, 张韧, 孙照渤. 2006. 基于交叉相关法的卫星云图中云团移动的短时预测. 中国图象图形学报, 11(4): 586–591

Liu Y A and Wei M. Application of FY-2C Data in Rainstorm Nowcasting. The First International Conference on Information Science and Engineering. 2009: 4766–4769 DOI: 10.1109/ICISE.2009.329

Mueller C, Saxen T, Roberts R, Wilson J, Betancourt T, Dettling S, Oien N and Yee J. 2003. NCAR Auto-Nowcast System. Weather and Forecasting, 18(4): 545–561 DOI: 10.1016/S0040-4020(97)10144–2

Vila D A, Machado L A T, Laurent H and Velasco I. 2008. Forecast and tracking the evolution of cloud clusters (ForTraCC) using satellite infrared imagery: methodology and validation. Weather and Forecasting, 23(2): 233–245 DOI: 10.1175/2007WAF2006121.1

Wilks D S. 2005. Statistical Methods in the Atmospheric Sciences: An Introduction. 2nd ed. Academic Press: 467